

SLS 2.0 MACHINE PROTECTION

F. Armbrust*, M. I. Besana, J. Kallestrup, M. Paraliev
Paul Scherrer Institut, 5232 Villigen PSI, Switzerland

Abstract

The machine protection architecture for the Swiss Light Source (SLS) 2.0 must fulfill more and tougher requirements than its predecessor for the SLS making it more complex and challenging to realise. The acceptable reaction time, the required emergency beam dump procedure with a dedicated beam dump and the sheer quantity of temperature sensors pose technical challenges for the realization of an effective and reliable machine protection architecture. This contribution introduces the current status of the planning for the overall machine protection architecture including details on the beam dump controller (BDC), the machine interlock system (MIS) and the foreseen emergency beam dump procedure.

INTRODUCTION

The beam abort system for the current SLS [1] is based on inverting the radio frequency (RF) phase to decelerate the stored beam. The subsequent losses are localised at longitudinal positions where the dispersive orbit encounters the machine aperture. For the SLS, these losses mainly occur at the septum and in the arcs. For the SLS 2.0 [2, 3] with its multi-bend-achromat (MBA) lattice and thus much lower dispersion in the arcs, tracking simulations show that these losses would occur 300 turns or $\sim 300\text{ }\mu\text{s}$ after the RF is switched off in a matter of $\sim 3\text{ }\mu\text{s}$. In case of an RF phase inversion the critical orbit is reached after just 100 turns. In both cases the losses would be localised at superconducting superbends [4] and in-vacuum insertion devices as shown in Fig. 1.

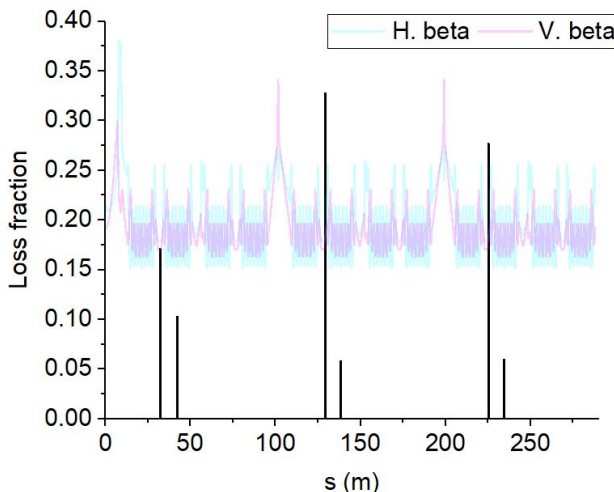


Figure 1: Beam loss distribution for the SLS 2.0 storage ring after turning off the RF. It is obtained with numerical tracking using elegant [5].

* felix.armbrust@psi.ch

Due to this unfortunate loss distribution, the fragile vacuum chamber with wall thicknesses down to 1 mm [6], the small beam size and the non-negligible stored beam energy of $\sim 1\text{ kJ}$, a fast and controlled emergency beam dump procedure is required. In case of an RF failure, the machine protection architecture (Fig. 2 shows an overview) must dump the beam safely before the critical dispersive orbit is reached. The majority of the surveilled sensors for triggering machine interlocks will be monitored by the slow, programmable-logic-controller (PLC) based MIS. Therefore, a fast beam dump controller with dedicated inputs for fast machine surveillance systems such as the low-level RF (LLRF) or the beam position monitor (BPM) system is foreseen for triggering the required emergency beam dump. For the MIS the sheer amount of monitored sensor signals poses a challenge.

MACHINE PROTECTION ARCHITECTURE

Machine Interlock System

The MIS has the task of monitoring a multitude of analogue and digital measuring circuits, the so-called input signals (sensors). The programming of the MIS PLC determines the output signals (actuators) based on the status of these sensors. The SLS 2.0 MIS combines the functionality of the magnet protection system (MPS) and MIS of the existing SLS. The most critical sensors are those triggering a beam dump. When their interlock threshold is reached, the corresponding actuator, e.g., "Emergency Beam Dump" is triggered. The MIS controlled actuators also include various enable signals for magnet power supplies and other PLC systems such as vacuum, front ends, beamlines and insertion devices.

The MIS is composed of 6 control racks in the inner technical gallery of which one is the head station with the CPU. The signals inside the tunnel are collected in 24 IO Boxes (2 per MBA section) connected to the control racks via Profinet. In total we expect ~ 300 actuator and ~ 6000 sensors-signals of which 80 % are analogue inputs. A simulation for the "most performant" Siemens CPU1518 which will be the workhorse for the SLS 2.0 MIS gives an expected PLC cycle time of 15 to 25 ms. The resulting, rather slow reaction time for the SLS 2.0 MIS gives the necessity to bypass the MIS and connect, e.g., the LLRF and BPM systems directly to the BDC. Extrapolating from experience with the SLS MIS with on average ~ 48 beam dumps per year between 2010 and 2022, we expect ~ 90 dumps per year triggered by the SLS 2.0 MIS considering the increased amount of sensor signals.

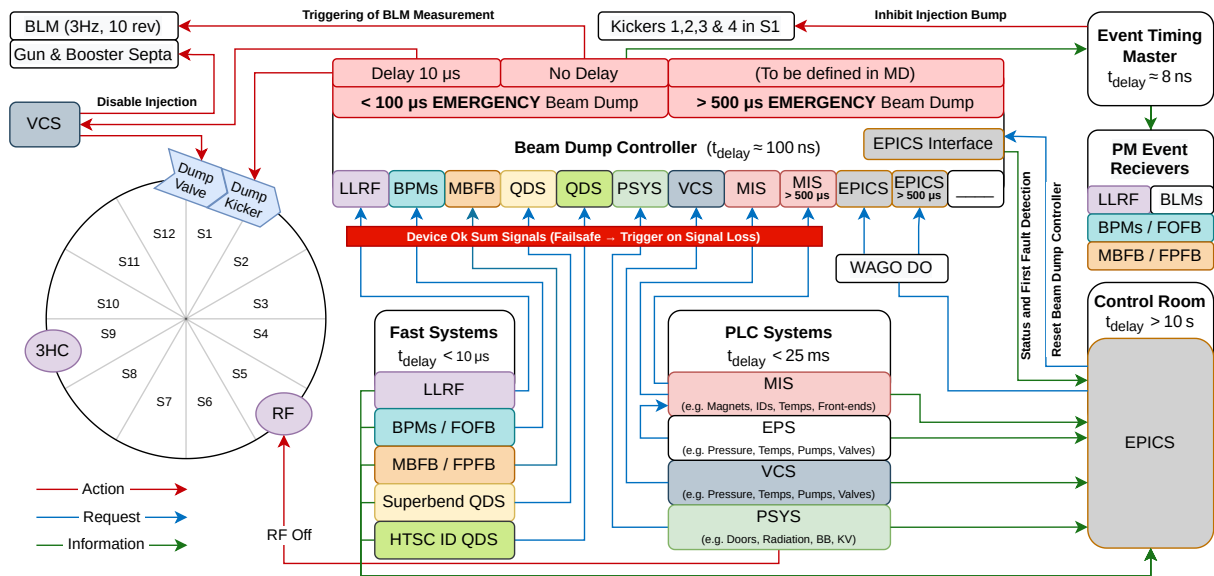


Figure 2: Overview of the SLS 2.0 machine protection architecture.

Beam Dump Controller

The main function of the BDC is combining the signals from all beam interlock systems and triggering the controlled emergency beam dump when required. After inhibiting the injection bump, the BDC triggers firing of the beam dump kicker, closing of the dump valve (backup) and disabling of the injector complex for the emergency beam dump. In addition, a measurement of the fast beam loss monitor (BLM) and the post mortem event are triggered. The main requirements for the BDC design were sufficiently fast reaction time for a safe beam dump in case of an RF trip, fail-safe logic, compatibility with a variety of systems and reliability. New features in comparison to the existing SLS beam dump controller triggering the RF phase inversion is the integration into the control system enabling post mortem archiving and first fault detection. The BDC registers all dump requests with relative arrival time for each emergency beam dump. This ordered list together with the post mortem data will help diagnosing the root cause of emergency beam aborts.

The time before a dispersive beam loss after an RF trip or phase inversion defines the required total BDC delay of $< 100 \mu\text{s}$. Critical systems requiring an emergency beam dump in less than 25 ms as specified by the MIS PLC bypass the MIS and directly trigger the BDC (see Fig. 2). The post mortem system will be implemented in the timing system and can also be triggered by other events besides the emergency beam dump.

Emergency Beam Dump

Initially it was foreseen to simply use the upstream tapering element and iron block of the thin septum as a beam dump. Considering the limited design flexibility for a combined beam dump and thin septum, it was decided to separate them also improving the potential issue of activation (see Table 1) in case of required interventions for the thin sep-

tum. A dedicated ~ 50 cm long copper beam dump will be installed as shown in Fig. 3 upstream of the magnetically shielded vacuum chamber next to the thick septum magnets.

Table 1: Expected loss distribution for regular operation of the SLS 2.0. The total values correspond to the fraction of lost particles at potential hot spots from emergency beam dumps ($\sim 90 \text{ a}^{-1}$) and finite lifetime due to Touschek losses ($\sim 18 \text{ h}$), Gas scattering ($\sim 35 \text{ h}$) and Bremsstrahlung ($\sim 90 \text{ h}$).

	Dump	Lifetime	Total
Beam losses per year	~ 90	~ 846	~ 488
At Collimators 9L	$< 1 \%$	22 %	38 %
At Collimators 5L	$< 1 \%$	14 %	24 %
At Thin Septum	8 %	11 %	21 %
At Beam Dump	86 %	—	16 %
At Thick Septum	5 %	—	21 %

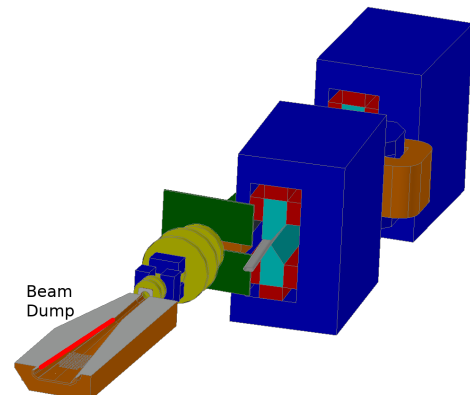


Figure 3: 3D drawing showing a cross section of the copper beam dump upstream of the thick septum. The red line indicates the distribution of dumped particles.

When the emergency beam dump is triggered, a dedicated beam dump kicker in the injection straight is fired and the entire beam is lost in $\sim 1 \mu\text{s}$. The kick varies along the bunch train, distributing the bunches horizontally on the beam dump as shown in Fig. 4. The first ~ 15 bunches of the 484 buckets accumulate two kicks. They are lost on the second turns at the dump. Of the following bunches the next ~ 6 hit the collimators, the next ~ 39 the thin septum, the next ~ 23 bunches the thick septum and finally all following bunches are distributed to the beam dump. A decoherence kick is not foreseen for the emergency beam dump. With a synchrotron frequency of $\sim 2.2 \text{ kHz}$ and chromaticity of ~ 1 it is difficult to reach adequate particle density reduction in under $100 \mu\text{s}$. A diluted beam dump might be implemented for less time critical dump triggers on the corresponding second output of the BDC. A dedicated dump valve is also closed for each emergency beam dump as a safety measure and backup. If the dump kicker fails the beam will be lost at this dedicated vacuum valve. Sacrificing a vacuum valve in this unlikely case is preferable over risking damage of in-vacuum-undulators or superconducting superbends. Immediate operation interrupting damage to the valve is not expected. The closed valve guarantees no current in the ring.

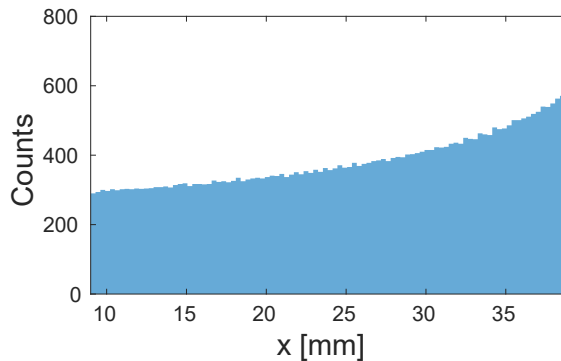


Figure 4: Tracking simulation [7] of uniform fill of 101 particles per bunch gives the loss distribution on the dedicated beam dump after firing the dump kicker with $7 \text{ kA} = 13.3 \text{ mrad}$ amplitude and $3.1 \mu\text{s}$ half-sine pulse duration.

An important topic for the beam dump is the deposited energy density (ED) and the corresponding instantaneous temperature rise. The beam size at the dedicated beam dump ($\sigma_{x/y} = 35/11 \mu\text{m}$) is smaller than at the thin septum ($\sigma_{x/y} = 58/9 \mu\text{m}$). Fortunately, the sharper angle of incidence, only feasible for the dedicated dump, reduces the surface ED in comparison to the thin septum beam dump by $\sim 33\%$ as shown in Table 2. The simulated ED peak is highly localized due to the small beam size. A fine mesh is required to resolve the peak values, as shown in Fig. 5. If the energy is averaged over larger bins, the estimated value is reduced by orders of magnitude. Therefore a sufficiently small grid size is important. Not considering the fusion energy (energy required for phase transition) and heat diffusion (negligible for $\sim 1 \mu\text{s}$), the acceptable deposited ED for copper without exceeding the melting temperature is $\sim 3.6 \text{ kJ cm}^{-3}$.

Table 2: Projected area of the transverse $1-\sigma$ beam size on the beam dump surface for both considered beam dump locations/geometries for perpendicular (\perp) and the actual geometric angle (\angle) of incidence. The percentages give the corresponding relative energy densities.

Angle	Thin Septum	Dedicated Dump
\perp	$1640 \mu\text{m}^2$ (100 %)	$1209 \mu\text{m}^2$ (140 %)
\angle	$5409 \mu\text{m}^2$ (30 %)	$9913 \mu\text{m}^2$ (20 %)

For a high-charge (5 nC) single bunch the deposited ED of $\sim 2.3 \text{ kJ cm}^{-3}$ is well below this limit. For the whole beam dump (400 mA), the kicker will spread the stored bunches over $\sim 331 \text{ mm}$ on the outer surface of the beam dump as shown in Fig. 5 with a maximum ED of $\sim 1 \text{ kJ cm}^{-3}$. Both the high charge single bunch and the whole beam dump give an instantaneous temperature rise well below the melting point of copper. Hence, no damage is expected. Dose simulations for the samarium-cobalt permanent magnets of the thick septum downstream of the dump give unproblematic values of 2.6 mJ cm^{-3} deposited energy or 0.33 Gy per beam dump.

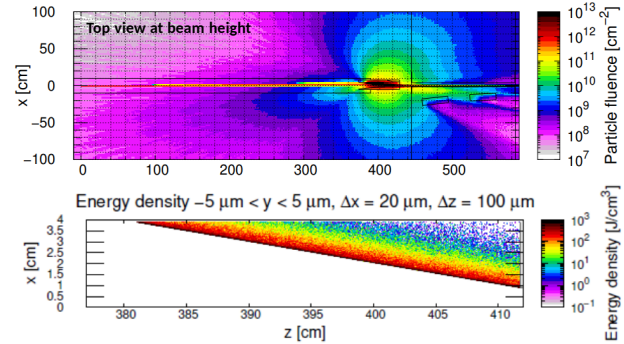


Figure 5: FLUKA [8–11] simulations for dumping 400 mA on the dedicated beam dump. The upper plot shows the particle fluence in of the dedicated beam dump design cross-sectioned at beam height. The lower plot shows the deposited ED on the surface of and inside the beam dump.

CONCLUSION

The machine protection architecture for the SLS 2.0 will be substantially faster and provide a more sophisticated emergency beam dump procedure and diagnostics in comparison to its predecessor. The challenges arising from the additional requirements are solved.

ACKNOWLEDGEMENTS

We gladly acknowledge the interesting discussions and support from our colleagues. Many thanks go to the SLS 2.0 project team and contributors to the machine protection subproject: M. Aiba, M. Böge, R. Ganter, A. Di Giovanna, C. H. Gough, A. Lüdeke, S. Müller, J. Snuverink, C. Stettler, X. Wang. Many thanks also to A. Lechner, F. Cerutti and F. S. Pujol from the CERN EN-STI-BMI section.

REFERENCES

- [1] M. Böge *et al.*, “The Swiss Light Source Accelerator Complex: An Overview”, in *Proc. EPAC'98*, Stockholm, Sweden, 1998, paper MOP28G, pp. 623–625.
- [2] H. Braun *et al.*, “SLS 2.0 Storage Ring. Technical Design Report”, PSI Report No. 21-02, 2021, <https://www.dora.lib4ri.ch/psi/islandora/object/psi:39635>.
- [3] R. Ganter *et al.*, “SLS 2.0 Storage Ring Components Overview Before Installation”, presented at IPAC'23, Venice, Italy, May 2023, paper MOPM020, this conference.
- [4] C. Calzolaio *et al.*, “Longitudinal Gradient Bend Magnets for the Upgrade of the Swiss Light Source Storage Ring”, in *IEEE Trans. App. Supercond.*, vol. 30, no. 4, pp. 1–5, Jun. 2020, art. no. 4100905. doi:10.1109/TASC.2020.2973113
- [5] M. Borland, “elegant: A Flexible SDDS-Compliant Code for Accelerator Simulation”, Argonne National Lab., IL, USA, Rep. LS-287, Aug. 2000. doi:10.2172/761286
- [6] R. Ganter *et al.*, “SLS 2.0 Vacuum Components Design”, presented at IPAC'23, Venice, Italy, May 2023, paper THPA147, this conference.
- [7] A. Terebilo, “Accelerator Modeling with MATLAB Accelerator Toolbox”, in *Proc. PAC'01*, Chicago, IL, USA, Jun. 2001, paper RPAH314, pp. 3203–3205.
- [8] G. Battistoni *et al.*, “Overview of the FLUKA code”, *Ann. Nucl. Energy*, vol. 82, pp. 10–18, 2015. doi:10.1016/j.anucene.2014.11.007
- [9] C. Ahdida *et al.*, “New Capabilities of the FLUKA Multi-Purpose Code”, *Front. Phys.*, vol. 9, art. no. 788253, 2022. doi:10.3389/fphy.2021.788253
- [10] V. Vlachoudis, “FLAIR: A Powerful But User Friendly Graphical Interface For FLUKA”, in *Proc. Int. Conf. on Mathematics, Computational Methods & Reactor Physics (M&C'09)*, Saratoga Springs, NY, USA May 2009, pp. 790–800.
- [11] FLUKA, <https://fluka.cern>.